

AD-A041 340

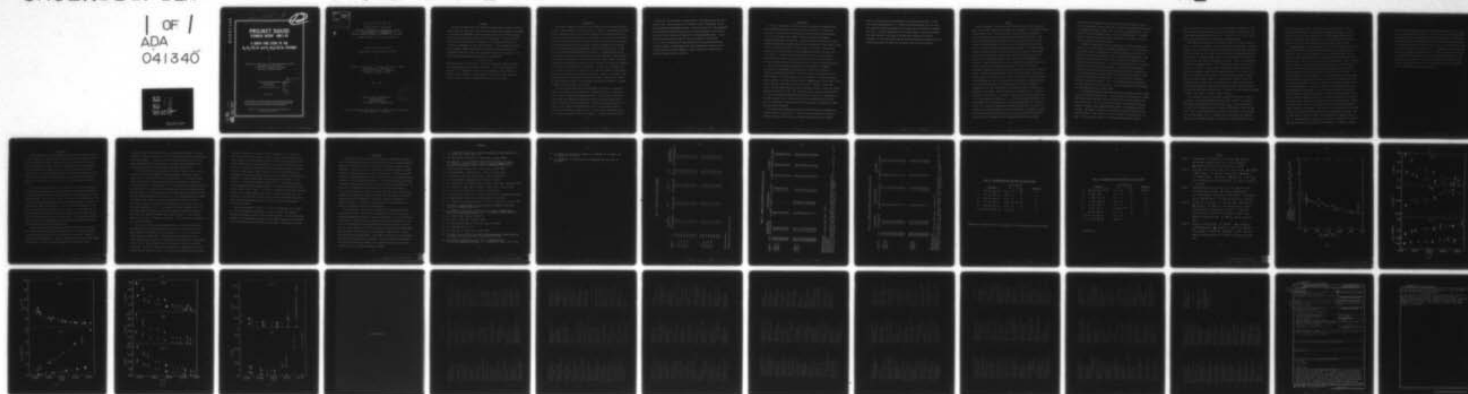
PURDUE UNIV LAFAYETTE IND PROJECT SQUID HEADQUARTERS F/G 7/4
A SHOCK TUBE STUDY OF THE H₂/O₂/CO/AR AND H₂/N₂O/CO/AR SYSTEMS. (U)
MAY 77 A M DEAN, D C STEINER, E E WANG N00014-75-C-1143

UNCLASSIFIED

SQUID-UM0-2-PU

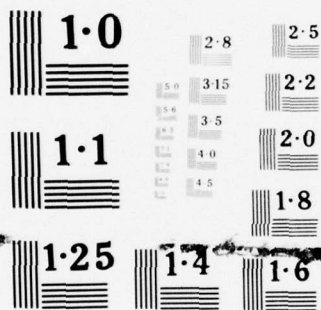
NL

1 OF 1
ADA
041340



END

DATE
FILMED
7-77



NATIONAL BUREAU OF STANDARDS
MICROCOPY RESOLUTION TEST CHART

ADA 041340

Lee 1473 *#* *12*

PROJECT SQUID

TECHNICAL REPORT UMO-2-PU

A SHOCK TUBE STUDY OF THE $H_2/O_2/CO/Ar$ and $H_2/N_2O/CO/Ar$ SYSTEMS

BY

ANTHONY M. DEAN, DON C. STEINER AND EDWARD E. WANG
DEPARTMENT OF CHEMISTRY
UNIVERSITY OF MISSOURI - COLUMBIA
COLUMBIA, MISSOURI 65201

PROJECT SQUID HEADQUARTERS
CHAFFEE HALL
PURDUE UNIVERSITY
WEST LAFAYETTE, INDIANA 47907

MAY 1977



Project SQUID is a cooperative program of basic research relating to Jet Propulsion. It is sponsored by the Office of Naval Research and is administered by Purdue University through Contract N00014-75-C1143, NR-098-038.

This document has been approved for public release and sale;
its distribution is unlimited

UJ NO. _____
UDC FILE COPY

ACCESSION for	
NTIS	White Section <input checked="" type="checkbox"/>
DDC	Buff Section <input type="checkbox"/>
UNANNOUNCED	<input type="checkbox"/>
JUSTIFICATION	
BY	
DISTRIBUTION/AVAILABILITY CODES	
ACCEL. and/or SPECIAL	

A

Technical Report UMO-2-PU

PROJECT SQUID

A COOPERATIVE PROGRAM OF FUNDAMENTAL RESEARCH
AS RELATED TO JET PROPULSION
OFFICE OF NAVAL RESEARCH, DEPARTMENT OF THE NAVY
CONTRACT N00014-75-C-1143, NR-098-038

A SHOCK TUBE STUDY OF THE
 $H_2/O_2/CO/Ar$ and $H_2/N_2O/CO/Ar$ SYSTEMS

BY

Anthony M. Dean, Don C. Steiner and Edward E. Wang
Department of Chemistry
University of Missouri - Columbia
Columbia, Missouri 65201

May, 1977

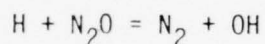
PROJECT SQUID HEADQUARTERS
CHAFFEE HALL
PURDUE UNIVERSITY
WEST LAFAYETTE, INDIANA 47907

DDC
RECEIVED
JUL 7 1977
D

This document has been approved for public release and sale;
its distribution is unlimited.

Abstract

Emissions at 450 nm and 4.27 μm have been measured when a variety of mixtures containing H_2 , CO, either O_2 or N_2O , and Ar were heated behind reflected shock waves to temperatures of 2000-2850 K and total concentrations near 5×10^{18} molecule/ cm^3 . These emissions were used to obtain absolute concentration - time data for both oxygen atoms and carbon dioxide. The data were then compared to the results of numerical integrations of the likely mechanisms. It was observed that quantitative agreement between calculations and observations were obtained for the $\text{H}_2/\text{CO}/\text{O}_2/\text{Ar}$ system using recent high temperature literature rate constants. For the $\text{H}_2/\text{CO}/\text{N}_2\text{O}/\text{Ar}$ system, the rate constant for the reaction:



was adjusted so as to fit the data. Here it was found that a good fit to both $[\text{O}]$ and $[\text{CO}_2]$ profiles could be achieved with $k = 3.0 \times 10^{-9} \exp(-113\text{kJ}/\text{RT}) \text{ cm}^3 \text{ molecule}^{-1} \text{ s}^{-1}$. Comparison to data at lower temperatures suggests that this might be another example of a "non-Arrhenius" rate constant. The implications of these results to studies of hydrocarbon oxidation are discussed.

INTRODUCTION

The study of oxidation reactions in shock tubes has been stimulated by the use of fast, accurate numerical integration routines. Now it is possible for kineticists to more definitively test various oxidation mechanisms by a detailed comparison of calculated and observed concentration - time profiles. The utility of the approach has been discussed by Schott and Getzinger [1] in their review of the H_2/O_2 system. Although the $H_2/O_2/CO$ system has also been successfully studied by this approach [2,3], extension to even simple hydrocarbon systems like CH_4/O_2 has been limited by lack of reliable high temperature rate constants. A common practice has been to extrapolate low temperature flow system data to the temperature range of interest. Unfortunately this approach can lead to serious errors; recent studies [4-10] have convincingly demonstrated that many reactions of importance in combustion mechanisms exhibit markedly "non-Arrhenius" rate constants. In this light it appears to be most desirable to measure rate constants in the same high temperature regime where they will be used to test the combustion mechanisms. However, it is equally important that these data be obtained from relatively simple systems where assignment of the desired rate constant is not contingent upon proper assignment of a complex mechanism and the associated rate constants.

One such system results from the substitution of N_2O for O_2 in combustion studies. Recent work in this laboratory [11] showed that N_2O is a particularly useful source of oxygen atoms between 2000-3000 K. Thus a study of combustion systems where N_2O replaced O_2 should provide useful information about rates of oxygen atom reactions at high temperatures. The primary advantage of N_2O as an oxidant is that oxygen atom reactions will occur in an environment where the concentration of molecular oxygen is much less than a normal combustion system; this considerably simplifies the kinetic analysis. Prudence dictates that such

a substitution first be tested on a known system. This paper reports the results of such a test. Data are given for an extensive series of experiments on both the $\text{H}_2/\text{O}_2/\text{CO}/\text{Ar}$ and $\text{H}_2/\text{N}_2\text{O}/\text{CO}/\text{Ar}$ systems. The results obtained in the $\text{H}_2/\text{O}_2/\text{CO}/\text{Ar}$ system coupled with those obtained earlier on N_2O dissociation serve to characterize most of the reactions of importance in the $\text{H}_2/\text{N}_2\text{O}/\text{CO}/\text{Ar}$ system. If the N_2O system profiles yield a value for the rate constant of the reaction $\text{O} + \text{H}_2 \rightarrow \text{OH} + \text{H}$ consistent with that obtained from the much more extensively studied O_2 system, it would suggest that the N_2O mechanism is appropriate and that N_2O substitution might indeed be a useful technique for obtaining high temperature oxygen atom rate constants.

EXPERIMENTAL

The 7.6 cm shock tube, gas handling system, and optical configuration have been described previously [11]. Infrared emissions were first collimated by two slits 1.5 mm wide and 5 mm high placed 50 mm apart before passing through a 4.27 μm interference filter (FWHM = 0.18 μm) and being focussed upon a liquid-nitrogen-cooled InSb detector. Visible emissions were monitored by a RCA 1P28A/V1 photomultiplier mounted behind a 450 nm interference filter (FWHM = 6.5 nm) and two 1 mm wide by 2 mm high slits 38 mm apart. The signals from the photomultiplier were collected with a Biomation Model 805 transient recorder at 0.5 μsec intervals. Infrared signals were monitored at 10.0 μsec intervals by a digital data acquisition system previously described [12]; the only change is that the Supernova computer has been replaced with a Motorola 6800 Microprocessor.

Gas mixtures were prepared manometrically using AIRCO Ar (99.9998%), CO_2 (99.999%), H_2 (99.9995%), and N_2O (99.995%), Scientific Gas Products O_2 (99.999%) and Matheson CO (99.99%). The CO was slowly passed through a coil of copper tubing at 77 K before addition to the vacuum line. The other gases were used as supplied. The shock tube was typically pumped down to 2 mPa (1.5×10^{-5} torr) with an observed leak-outgassing rate of less than 2.5 mPa/min. Shocks were usually initiated approximately one minute after pump isolation so that the nominal background pressure was 5 mPa. The initial test section pressures were typically 2.7 kPa so that background impurities contributed ~ 2 ppm which is comparable to the total impurity levels in the mixtures used. Helium was used as the driver gas in all experiments, and shocks were initiated by either spontaneous or manual rupture of Mylar diaphragms.

No-reaction shock conditions behind the reflected shock were obtained from measured incident shock velocities. There was little difference in conditions calculated using a constant velocity assumption and those where the measured

(small) velocity changes were extrapolated to the observation window. Usually these methods agreed within 25 K. Shocks which had differences of 50 K or more were rejected. Conditions reported in this paper used the assumption of constant velocities. Pressures computed with this assumption were in very good agreement with those measured in the plane of the observation windows by a pressure transducer. No corrections were made for non-ideal effects; the observed pressure profiles were always flat over the time interval that data were collected.

RESULTS

Visible Emissions. Systems containing oxygen atoms and carbon monoxide are known to emit visible radiation whose intensity is proportional to the concentrations of these species [13]. In these experiments this emission was monitored at 450 nm to attempt to minimize the contribution of extraneous emissions. This system was calibrated using the partial-equilibrium technique [13]. Here two mixtures of $H_2/O_2/CO/CO_2/Ar$ (See Table I) were heated behind reflected shock waves to 1970-2745 K and the flame-band emission recorded. This signal rapidly reached a constant intensity which was maintained for hundreds of microseconds. This constant signal arises from the quasi-equilibrium concentrations of the various species (including radicals) prior to the onset of recombination reactions. These concentrations are easily calculated from the well known equilibrium constants of the bimolecular reactions of interest. Note these experiments were done at relatively low total concentrations to minimize recombination. The observed constant signal and the fact that variation of the total concentration by a factor of two had no effect upon the signal levels were taken as evidence that the effect of recombination was negligible. Additional experiments near 5×10^{18} molecule/cm³ indicated small but noticeable deviations suggesting that at that concentration the assumption of partial equilibrium is beginning to break down. The least square fit to the data in Fig. 1 yields an activation energy of 16.9 ± 2.7 kJ/mole. This can be compared to the value of 14.4 kJ/mole reported by Schott, et. al., [13] over the range 1300-2000 K. The data suggests this calibration factor is good to approximately 10%. With this factor, it is possible to determine the product $[CO][O]$ over the temperature interval by a simple measurement of the flame-band signal. Attempts to use this data to determine oxygen atom concentrations are complicated by the fact that there will be small changes in the CO concentration during an experiment.

To eliminate this ambiguity, the calibration factor was incorporated into the numerical integration scheme and was used to convert the computed $[CO][O]$ product to a computed flame-band voltage. This could then be compared directly to that observed; note this procedure allows for no normalization factors. In effect, given the small CO concentration changes (typically on the order of 5%) this approach yields absolute O-atom profiles.

Although the wavelength chosen for observations minimized the background emissions, it was not possible to completely eliminate them. For this reason, a preliminary series of experiments were performed which were similar in all respects to those listed in Tables II and III except that CO was omitted. Here the time-resolved emissions at 450 nm were recorded over a temperature range somewhat larger than that listed. This background data was fed into a two-dimensional array in the data reduction program. A bicubic spline interpolation routine was used to estimate the time-varying background at the temperature of a "real" experiment and this background was then subtracted from the total signal to yield the corrected flame-band signal. It was estimated the background obtained in this way was good to $\sim 10\%$. The background for the O_2 experiments was much smaller than for the N_2O shocks. Even for the N_2O case, the background was typically only 10% of the total signal.

In the N_2O experiments the flame-band signal was observed to increase rapidly upon passage of the reflected shock. In many instances the increase was so rapid that the observed signal was clearly affected by the finite slit width of the observation system. The slit effect was included in the numerical integration scheme by integrating the computed $[CO][O]$ product over the appropriate slit function. The detector efficiency was assumed to be unity for the 1.0 mm slit opening and then to drop linearly to zero at a distance 2.3 mm beyond each slit edge. In this way, the computed slit-modified flame-band signal could be

directly compared to that observed. Here it was convenient to define t_0 as the time at which the reflected shock front was first visible to the detector. All visible data are reported with respect to t_0 . Typically, t_0 is ~ 5 μ sec earlier than t_{mp} , the time of shock front passage of the window midpoint.

Experimental observations of the flame-band signals are listed in Tables II and III. For the O_2 experiments, induction times were clearly evident. Here the induction time t_i is defined as the time at which the corrected flame-band signal equals 20 mv, which was the lowest signal which could be reproducibly extracted from the data. As one would expect, the t_i values for Mixture D are lower than those of C since here the CO concentration was larger. For C, t_i corresponds to an oxygen atom concentration of $\sim 1 \times 10^{15}$ molecule/cm³; whereas in D the concentration is $\sim 2.5 \times 10^{14}$. In D the higher CO concentration made it possible to observe the exponential growth of the flame-band emission. In all cases it was possible to observe at least a decade of such growth and the slopes of these plots are listed in Table II where λ is defined as the slope of a plot of \ln (flame-band signal) versus time. Similar plots for C yielded curves that were clearly concave downward, indicating the exponential growth region occurred at concentrations below the sensitivity level. At later times both mixtures exhibited a constant signal which is listed in Table II as V_{max} .

The flame-band signals from the N_2O system were characterized in terms of $t_{1/2}$ and V_{max} . Here $t_{1/2}$ was defined as the time (again relative to t_0) when the signal had reached one-half its plateau value of V_{max} . As one would expect, the nature of the flame-band signal is drastically different in the O_2 and N_2O cases. Figs. 2 and 3 illustrate this difference. Note that $t_{1/2}$ values for N_2O are even lower than t_i for O_2 . Qualitatively such differences are expected; the oxygen atom concentration gets a "head start" in the N_2O system since N_2O

dissociation is faster than the initiation reactions in the O_2 case. Also note the marked difference in the temperature dependencies of V_{\max} . In these figures the error bars were computed with a standard propagation scheme and included contributions from uncertainties in the calibration (10%), background corrections (10%), and the measurement of the flame-band signal (5-10%).

Infrared Emissions. The total signal at $4.27 \mu m$ was corrected for emissions other than those due to CO_2 with a procedure similar to that used for the visible signal. Here a series of $N_2O/CO/Ar$ as well as CO/Ar experiments were performed to determine the background. The corrected time-resolved data were then converted to CO_2 profiles via calibration factors obtained from a series of CO_2/Ar shocks. Parameters used to characterize these profiles are listed in Tables II and III. It was observed in both the N_2O and O_2 systems that the first data collected were at sufficiently long times to ignore possible slit effects. For ease of comparison to the calculations, all times recorded for the infrared data are with respect to t_{mp} , the time when the reflected shock reached the midpoint of the observation window. Note this convention is different from that used for the visible data where t_0 was used. In general the CO_2 profiles for the O_2 system exhibited an induction time, quickly achieved a region of linear growth, and then gradually approached a constant (or slightly increasing) value. There was not sufficient temporal resolution to accurately characterize the region of increasing rate or the period of constant rate. The induction time was defined in the usual way as the t -axis intercept of the line which passed through the points exhibiting linear growth. Later points on the profile were characterized in terms of the time at which a particular CO_2 concentration was reached. Two of these times are listed in Table II and shown along with induction times in Fig. 4. The CO_2 profiles in the N_2O system were also characterized in terms of the times required to reach certain CO_2 concentrations. In general, CO_2 pro-

duction in the N_2O system was much more rapid than that observed in the O_2 system; no induction period was evident. At longer times, the CO_2 concentrations were generally smaller in the N_2O system than in the O_2 work. The differences were most pronounced at higher temperatures and in the 3% CO mixtures where the concentrations were lower by about a factor of three. The characteristic times are listed in Table III and shown in Fig. 5. In both Figs. 4 and 5, the error bars were calculated assuming 10% errors in the CO_2 calibration, 10% error in the background correction, and 1-5% error in the observed signal. The large error bars in some regions of Figs. 4 and 5 are due to the relatively small slopes in those particular profiles at certain times; here small calibration errors translate into large time uncertainties.

DISCUSSION

A likely mechanism for the $\text{H}_2/\text{O}_2/\text{CO}/\text{Ar}$ system includes the reactions listed in Table IV [2,14]. Fortunately the rate constants for many of these reactions have been extensively studied. Perhaps the most interesting result of recent work is the growing consensus that the high temperature measurements yield rate constants higher than one would expect by a simple extrapolation of the low temperature data. Thus an attempt was made to see if the above mechanism, using rate constants determined at high temperatures, was quantitatively consistent with the data reported herein. Table IV lists the rate constants used for this purpose.

This system of equations with the associated rate constants was numerically integrated using a program previously described [17]. The program was modified to use the flame-band calibration data to convert the $[\text{CO}]$ $[\text{O}]$ product to a corresponding voltage. The slit effect was also calculated as described earlier. The calculated flame-band and CO_2 profiles were then treated exactly as the experimental data to yield calculated values of the various reaction parameters. Results of the calculations are shown in Figs. 2 and 4. It is felt that the extent of agreement can be taken as additional evidence for the essential correctness of the mechanism and the rate constants chosen. It was particularly gratifying to observe such good agreement on an absolute scale for both observables over the entire time range of the observations.

Sensitivity tests were performed by varying the individual rate constants by a factor of two each way and observing the effect on the computed profiles. It was seen that this system is most sensitive to k_2 , k_4 , and k_5 . Changes in one of these must be offset by a change in another to keep the calculations within the error bars. Since k_2 and k_4 were determined on systems where k_5 was

not involved, and the determination of k_5 was done under conditions to minimize the effect of other rate constants, there is clearly no justification for modifying these rate constants. It should be noted that the value used here for k_5 is in quite good agreement with that proposed in a recent review [7] and that k_2 and k_4 were obtained from an extensive study of the H_2/O_2 system [13,16].

A likely mechanism for the N_2O system is listed in Table V. This is similar to that used earlier for $N_2O/H_2/Ar$ systems [18-20] with the addition of the reactions of CO. Of particular note is that Reactions 1' - 3' have been studied under simpler conditions where specification of rate constants is relatively straightforward [11,21]. Also Reactions 2 - 6 can be carried over directly from the O_2 system where it was explicitly verified that these values were consistent with the present data. In this sense, one can approach the N_2O system with essentially only one unknown, namely the rate constant k_4' . Thus the approach taken was simply to attempt to find a value of k_4' which was compatible with all of the data. Preliminary calculations showed that the profiles were very sensitive to k_1' and very slight adjustments in k_1' ($\sim 10\%$ change from the value reported in Ref. 11) noticeably improved both the V_{max} temperature dependence and the CO_2 profiles. Such a shift was compatible with the data reported in Ref. 11. This adjusted value of k_1' was used in subsequent calculations. These calculations now treated k_4' as the only variable.

There is very little high temperature data on k_4' ; only one study [18] has reported values for temperatures above 2000 K [22]. Recently this reaction has been studied in a flow system over the interval $718\text{ K} \leq T \leq 1111\text{ K}$ [23] and in flames between 1000-1700 K [24]. The reported activation energies for this lower temperature work range from 55 kJ/mole [24] to 72 kJ/mole [23]; extrapolation of these results into the higher temperature regime thus leads to considerable uncertainty. A series of calculations suggested that the value obtained by extrapolating the flow tube work to 2450 K was in quite good accord with our data, but

that obvious problems were apparent at higher temperatures. In particular, calculated values of the flame-band plateau (V_{\max}) were too high and there was a severe mismatch in the long time CO_2 profiles. Both of these features were improved significantly in both N_2O mixtures by increasing the value of k_4' by 50% at 2900 K. Furthermore, the overall temperature dependence of V_{\max} is improved by using a value of k_4' at 2100 K somewhat lower than that obtained from an extrapolation of k_4' from the flow tube work. For this reason a value of k_4' was obtained by a simple pivoting about the extrapolated value at 2450 K. This yields $k_4' = 3.0 \times 10^{-9} \exp(-113\text{kJ/RT}) \text{ cm}^3 \text{ molecule}^{-1} \text{ s}^{-1}$. Note this expression is only applicable over the range 1950-2850 K. The agreement obtained with this value is shown in Figs. 3 and 5. In addition it should be mentioned that detailed comparisons of computed profiles with particular experiments showed (in a vast majority of cases) that the calculated values for both flame-band and CO_2 signals were within the experimental error bars for the entire 500 μsec observation time for both mixtures.

The value reported here from k_4' is in very good agreement (14%) at 2000 K with the value suggested by Leeds [22]. However, at 2900 K this value has increased to be nearly a factor of three larger than Leeds. Such an increase was mandated by the observations, and this fact may indeed suggest that this reaction is one more addition to those recently discovered with "non-Arrhenius" behavior.

CONCLUSIONS

In this work emission signals have been related to the absolute concentration - time behavior of oxygen atoms and carbon dioxide over an extended range of conditions. These data provide a crucial test for any mechanism/rate constant combination. The ability of such a combination to accurately model all of these data would strongly suggest such a scheme is appropriate. In the O_2 system the mechanism is generally accepted and thus it was possible to test the best current estimates of the associated rate constants. The agreement observed can be taken as rather convincing evidence of the correctness of the rate constants used. In particular it reinforced the earlier observations that both the reactions $O + H_2 \rightarrow OH + H$ and $OH + CO \rightarrow CO_2 + H$ have rates well above what a simple extrapolation of low temperature data would suggest. This observation is critically important when one is attempting to choose rate constants for modeling of a combustion system; it is imperative that one be aware of the difficulties inherent in using data collected at low temperatures.

For the N_2O case it was possible to approach the system with most of the rate constants in hand. After a value was obtained for $H + N_2O \rightarrow OH + N_2$, no further adjustments were required to obtain a quantitative fit to the observations. In particular, it was observed that the profiles were quite sensitive to $O + H_2 \rightarrow OH + H$ and that the best fit was obtained with the same value which fit the O_2 system. In this respect it is felt this sequence of experiments has demonstrated that substitution of N_2O for O_2 is a useful method to measure rates of oxygen atom reactions at high temperatures. Furthermore, it appears that the postulated mechanism for the N_2O system is reasonable. This point should be very useful in the analysis of ongoing experiments in this laboratory where N_2O is being substituted for O_2 in a variety of combustion systems.

REFERENCES

1. G.L. Schott and R.W. Getzinger, in Physical Chemistry of Fast Reactions, Vol. 1, B.P. Levitt, Ed., Plenum, 1973, p.81.
2. A.M. Dean and G.B. Kistiakowsky, J. Chem. Phys., 53, 830 (1970).
3. W.C. Gardiner, Jr., W.G. Mallard, M. McFarland, K. Morinaga, J.H. Owen, W.T. Rawlins, T. Takeyama, and B.F. Walker, Fourteenth Symposium (International) on Combustion, Combustion Institute, Pittsburgh, 1973, p.61.
4. R. Zellner and W. Steinert, Int. J. Chem. Kinet., 8, 397 (1976).
5. R.N. Dubinsky and D.J. McKenney, Can. J. Chem., 53, 3531 (1975).
6. P. Roth and Th. Just, Ber. Bunsen. Physik. Chem., 79, 682 (1975).
7. D.L. Baulch and D.D. Drysdale, Comb. Flame, 23, 215 (1974).
8. W.C. Gardiner, Jr., W.G. Mallard, and J.H. Owen, J. Chem. Phys., 60, 2290 (1974).
9. J.C. Biordi, J.F. Papp, and C.P. Lazzara, J. Chem. Phys., 61, 741 (1974).
10. T.C. Clark and J.E. Dove, Can. J. Chem., 51, 2147 (1973).
11. A.M. Dean and D.C. Steiner, J.Chem. Phys., 66, 598 (1977) and references therein.
12. R. Megargle and A.M. Dean, Chem. Instrumentation, 5, 109 (1973).
13. G.L. Schott, R.W. Getzinger, and W.A. Seitz, Int. J. Chem. Kinet., 6, 921 (1974).
14. R.S. Brokaw Eleventh Symposium (International) on Combustion, Combustion Institute, Pittsburgh, 1967, p.1063.
15. D.L. Baulch, D.D. Drysdale, D.G. Horne, and A.C. Lloyd, Evaluated Kinetic Data for High Temperature Reactions, Vol. 1, Butterworth, London, 1972, p.77.
16. G.L. Schott, Comb. Flame 21, 357 (1973).
17. A.M. Dean, J. Chem. Phys., 58, 5202 (1973).
18. H. Henrici and S.H. Bauer, J. Chem. Phys., 50, 1333 (1969).
19. R.I. Soloukhin, Ref. 3, p. 77.
20. A.M. Dean, Int. J. Chem. Kinet., 8, 459 (1976).
21. J.E. Dove, W.S. Nip, and H. Teitelbaum, Fifteenth Symposium (International) on Combustion, Combustion Institute, Pittsburgh, 1975, p. 903.
22. D.L. Baulch, D.D. Drysdale, and D.G. Horne, Evaluated Kinetic Data for High Temperature Reactions, Vol. 2, Butterworth, London, 1973, p.453.

23. E.A. Albers, K. Hoyer mann, H. Schacke, K.J. Schmatjko, H. Gg. Wagner, and J. Wolfrum, Ref. 21, p. 765.
24. V.P. Balakhnine, J. VanDooren, and P.J. VanTiggelen, Comb. and Flame, 28, 165 (1977).

TABLE I. FLAME-BAND CALIBRATION EXPERIMENTS

Mixture ^a	T	Total Concentration (10 ¹⁸ molec/cm ³)	[O] _{P.E.} ^b (10 ¹⁶ molec/cm ³)	[CO] _{P.E.} ^b (10 ¹⁷ molec/cm ³)	Signal (Volts)	Signal $\frac{[O]_{P.E.} [CO]_{P.E.}}{(10^{-34} \text{ V cm}^6 \text{ molec.}^{-2})}$
A	2035	1.44	1.56	1.70	0.37	1.39
	2245	1.52	1.65	1.86	0.45	1.47
	2260	1.53	1.66	1.87	0.49	1.58
	2345	1.51	1.64	1.87	0.48	1.57
	2470	1.51	1.63	1.89	0.55	1.78
	2540	1.57	1.68	1.99	0.56	1.66
	2670	1.52	1.63	1.93	0.54	1.72
	2690	1.56	1.69	1.99	0.61	1.81
B	1970	2.52	1.36	1.45	0.30	1.52
	2060	2.66	1.44	1.56	0.31	1.38
	2205	2.74	1.48	1.64	0.36	1.48
	2230	2.82	1.53	1.70	0.38	1.46
	2415	2.80	1.50	1.73	0.43	1.65
	2475	3.07	1.64	1.90	0.49	1.56
	2620	2.98	1.57	1.88	0.51	1.74
	2745	2.75	1.43	1.74	0.51	2.05

^aBalance was Argon.^bComputed partial-equilibrium values.

TABLE II. SUMMARY OF EXPERIMENTAL OBSERVATIONS (O₂ SYSTEM)

Mixture ^a	T(K)	Concentration (10 ¹⁸ molec/cm ³)	t_i (μ sec) ^b	Flame-Band Signal λ (μ sec ⁻¹) ^c	V_{max} (volts) ^d	t_i (μ sec) ^e	CO ₂ Signal t' (μ sec) ^f	t'' (μ sec) ^g
C 0.049% H ₂ 1.01% O ₂ 3.28% CO	2050	4.42	136	-	0.44	130	195	375
	2140	4.52	107	-	0.49	102	165	320
	2250	4.60	75	-	0.54	75	120	237
	2355	4.69	66	-	0.56	62	105	225
	2560	4.84	43	-	0.70	39	64	126
	2620	4.87	36	-	0.71	35	57	115
	2675	4.95	32	-	0.72	34	55	112
	2765	4.96	26	-	0.76	24	44	94
	2810	4.99	25	-	-	26	46	100
D 0.050% H ₂ 1.00% O ₂ 12.17% CO	2070	4.95	57	.073	3.1	78	108	185
	2160	5.07	47	.100	3.3	60	84	143
	2215	5.10	43	.108	3.4	54	78	137
	2215	5.11	38	.089	3.5	53	76	130
	2325	5.21	26	.109	3.8	42	58	98
	2375	5.24	27	.110	3.8	41	58	100
	2475	5.34	16	.110	4.1	32	45	80
	2565	5.38	16	.149	4.3	29	42	75
	2625	5.45	15	.164	4.5	23	35	60
	2700	5.49	12	.160	4.4	23	35	63
	2740	5.55	5	.144	4.5	16	27	50
	2820	5.55	4	.154	4.8	17	26	48
	2870	5.63	11	-	5.0	15	24	45

^aBalance was Argon.^bTime relative to t_0 (see text) when signal = 0.02V.^c $d \ln(\text{signal})/dt$ ^dPlateau signal.^eTime relative to t_{mp} (see text) at which tangent to [CO₂]-time plot intercepts t -axis.^fFor Mixture C, time relative to t_{mp} (see text) when [CO₂] = 8.0×10^{15} molec/g/cm³. For D, time when [CO₂] = 1.0×10^{16} .^gFor C, time (see f) when [CO₂] = 2.4×10^{16} . For D, time when [CO₂] = 3.0×10^{16} .

TABLE III. SUMMARY OF EXPERIMENTAL OBSERVATIONS (N₂O SYSTEM)

Mixture ^a	T(K)	Concentration (10 ¹⁸ molec./cm ³)	Flame-Band Signal		CO ₂ Signal	
			t _{1/2} (μsec) ^b	V _{max} (volts) ^c	t' (μsec) ^d	t'' (μsec) ^e
E 0.050% H ₂ 1.01% N ₂ O 2.99% CO	1930	4.39	98	.09	72	123
	2045	4.49	39	.11	46	90
	2090	4.56	28	.13	38	77
	2150	4.57	22	.18	18	55
	2255	4.69	15	.24	20	47
	2285	4.70	22	.24	23	52
	2380	4.79	15	.32	12	43
	2440	4.83	16	.38	13	50
	2470	4.96	14	.45	13	40
	2545	4.89	12	.44	8	40
	2635	4.95	8	.58	--	70
	2750	5.08	9	.64	11	140
	2765	5.05	10	.60	12	180
F 0.049% H ₂ 1.04% N ₂ O 12.01% CO	2030	4.95	32	.50	30	71
	2065	5.01	31	.73	25	58
	2210	5.19	20	1.10	15	42
	2235	5.18	15	1.35	13	35
	2305	5.22	19	1.45	14	37
	2360	5.32	15	1.72	11	37
	2420	5.38	12	1.95	10	33
	2535	5.48	10	2.25	8	75
	2605	5.54	9	2.70	9	118
	2720	5.63	7	3.10	8	250
	2845	5.70	7	3.90	6	235

^aBalance was Argon.

^bTime relative to t₀ (see text) when signal = 1/2 plateau value.

^cPlateau signal.

^dFor Mixture E, time relative to t_{mp} when [CO₂] = 4x10¹⁵ molecules/cm³. For F, time when [CO₂] = 5x10¹⁵.

^eFor Mixture E, time relative to t_{mp} when [CO₂] = 1.0x10¹⁶. For F, time when [CO₂] = 2.0x10¹⁶.

TABLE IV. MECHANISM AND RATE CONSTANTS FOR THE O₂ SYSTEM

	Reaction	Rate Constant ^a		Reference
		A	E _a	
1.	CO + O ₂ = CO ₂ + O	5.8 E - 12	210	2
2.	O + H ₂ = OH + H	3.6 E - 10	57	13
3.	OH + H ₂ = H ₂ O + H	3.6 E - 11	22	15
4.	H + O ₂ = OH + O	2.0 E - 07 T ^{-.91}	70	16
5.	OH + CO = CO ₂ + H	6.7 E - 12	33	3
6.	CO + O + M = CO ₂ + M	1.6 E - 34	0	11

^aExpressed in Arrhenius form, $k = A \exp(-E_a/RT)$, A in cm-molecule-sec units, E_a in kJ/mol.

TABLE V. MECHANISM AND RATE CONSTANTS FOR THE N_2O SYSTEM

	Reaction	Rate Constant ^a		Reference
		A	E _a	
1'	$N_2O + M = N_2 + O + M$	$2.7 \text{ E} - 10$	216	See text
2'	$O + N_2O = 2NO$	$7.7 \text{ E} - 11$	117	11
3'	$O + N_2O = N_2 + O_2$	$7.7 \text{ E} - 11$	117	11
2	$O + H_2 = H_2O + H$	$3.6 \text{ E} - 10$	57	13
3	$OH + H_2 = H_2O + H$	$3.6 \text{ E} - 11$	22	15
4	$H + O_2 = OH + O$	$2.0 \text{ E} - 07 \text{ T}^{-.91}$	70	16
5	$OH + CO = CO_2 + H$	$6.7 \text{ E} - 12$	33	3
6	$CO + O + M = CO_2 + M$	$1.6 \text{ E} - 34$	0	11
4'	$H + N_2O = N_2 + OH$	See text		

^aSee Table IV.

LEGENDS

- Figure 1. Arrhenius plot of flame-band calibration data. \bullet = Mixture A; here the total concentration was near 1.5×10^{18} molecule/cm³. \blacksquare = Mixture B; here the concentration was near 2.9×10^{18} .
- Figure 2. Flame-band data for the O₂ system. (a) Induction Times: \bullet = Mixture C; \blacksquare = Mixture D. (b) Exponential Growth Rates: \blacksquare = Mixture D. (c) Plateau Voltages: \bullet = Mixture C; \blacksquare = Mixture D. In all cases, the solid symbols are the calculated values. All times are relative to t₀ (see text).
- Figure 3. Flame-band data for the N₂O system. (a) Time required to reach one-half the plateau voltage: \bullet = Mixture E; \blacksquare = Mixture F. (b) Plateau Voltages: \bullet = Mixture E; \blacksquare = Mixture F. Solid symbols are the calculated values. All times are relative to t₀ (see text).
- Figure 4. CO₂ data for the O₂ system. (a) Induction Times: \bullet = Mixture C; \blacksquare = Mixture D. (b) Mixture C: Δ = time when [CO₂] = 8.0×10^{15} molecule/cm³; ∇ = time when [CO₂] = 2.4×10^{16} . (c) Mixture D: Δ = time [CO₂] = 1.0×10^{16} ; ∇ = time [CO₂] = 3.0×10^{16} . Solid symbols are calculated values. All times are relative to t_{mp} (see text).
- Figure 5. CO₂ data for the N₂O system. (a) Mixture E: \bullet = time [CO₂] = 4.0×10^{15} molecule/cm³; \blacksquare = time [CO₂] = 1.0×10^{16} . (b) Mixture F: Δ = time [CO₂] = 5.0×10^{15} ; ∇ = time [CO₂] = 2.0×10^{16} . The solid symbols are calculated values. All times are relative to t_{mp} (see text).

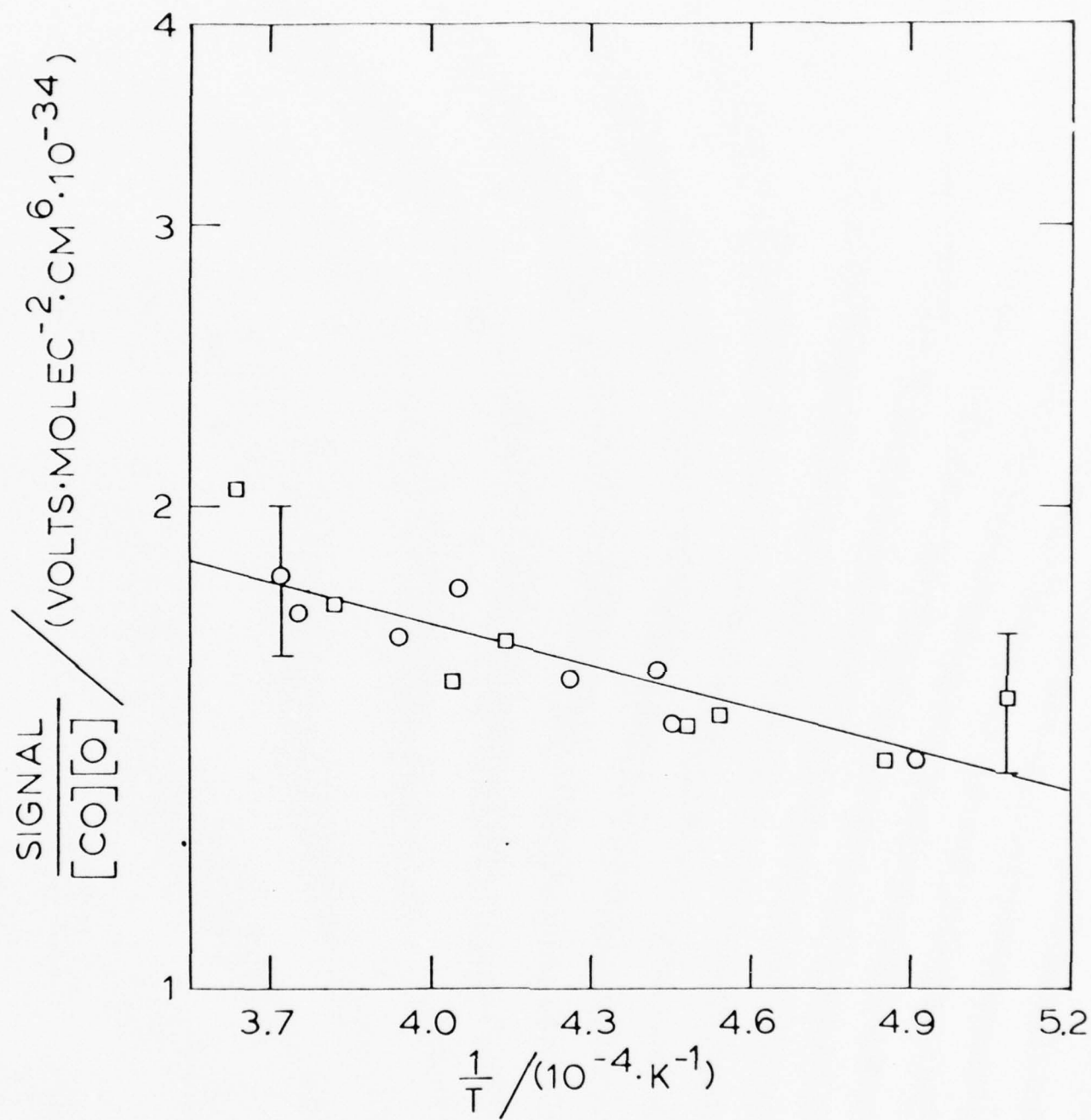


Fig. 1

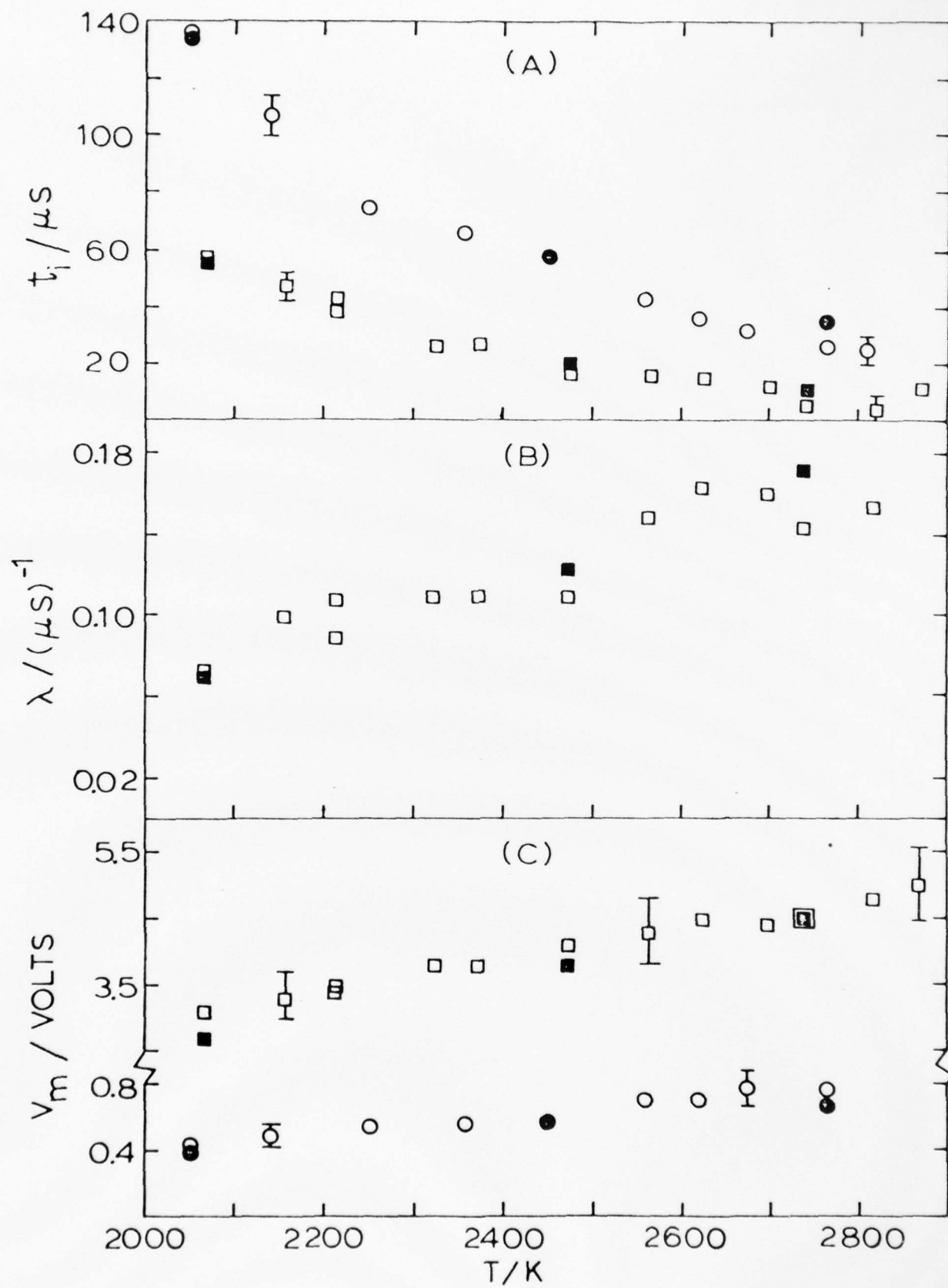


Fig. 2

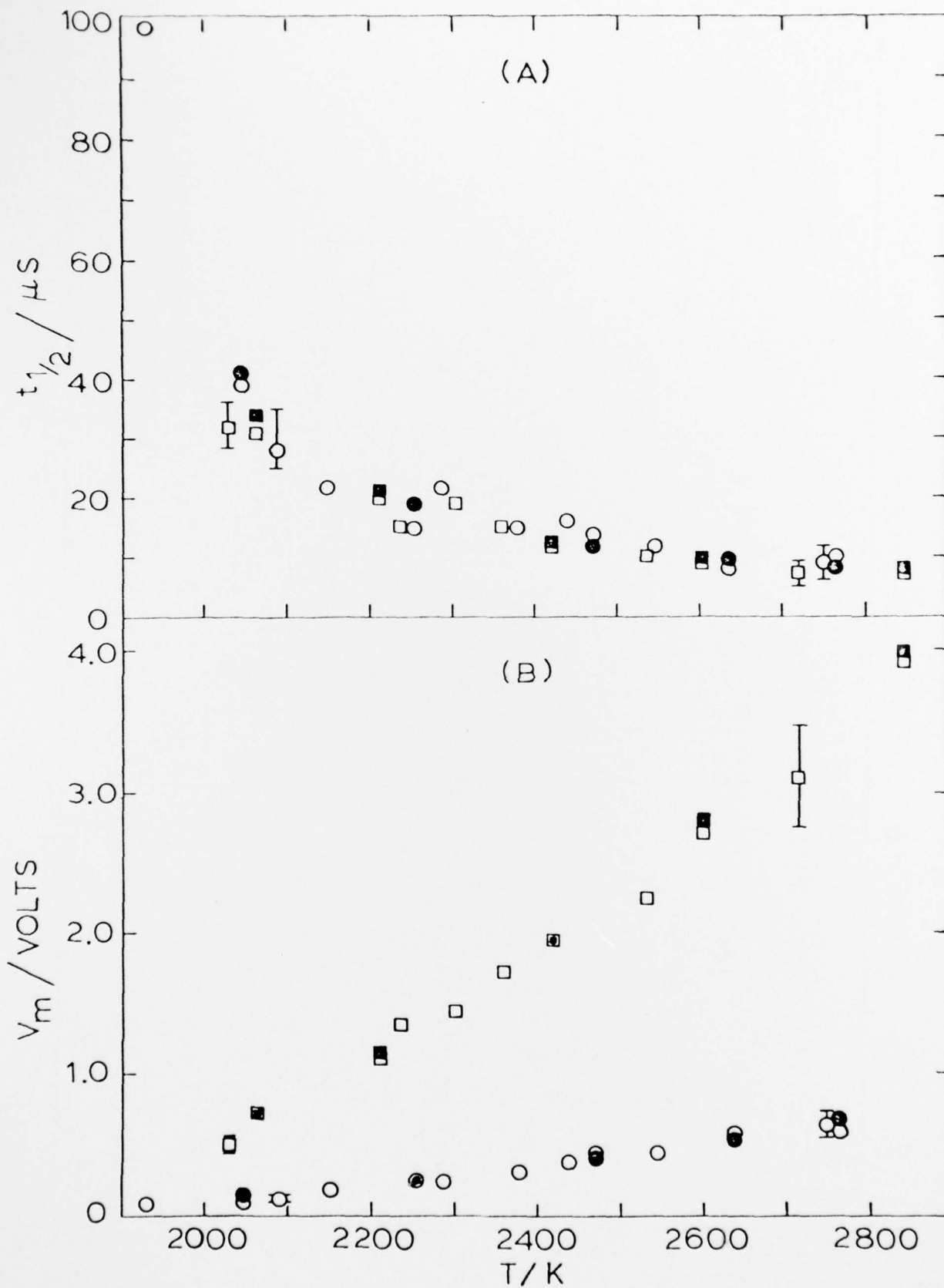


Fig. 3

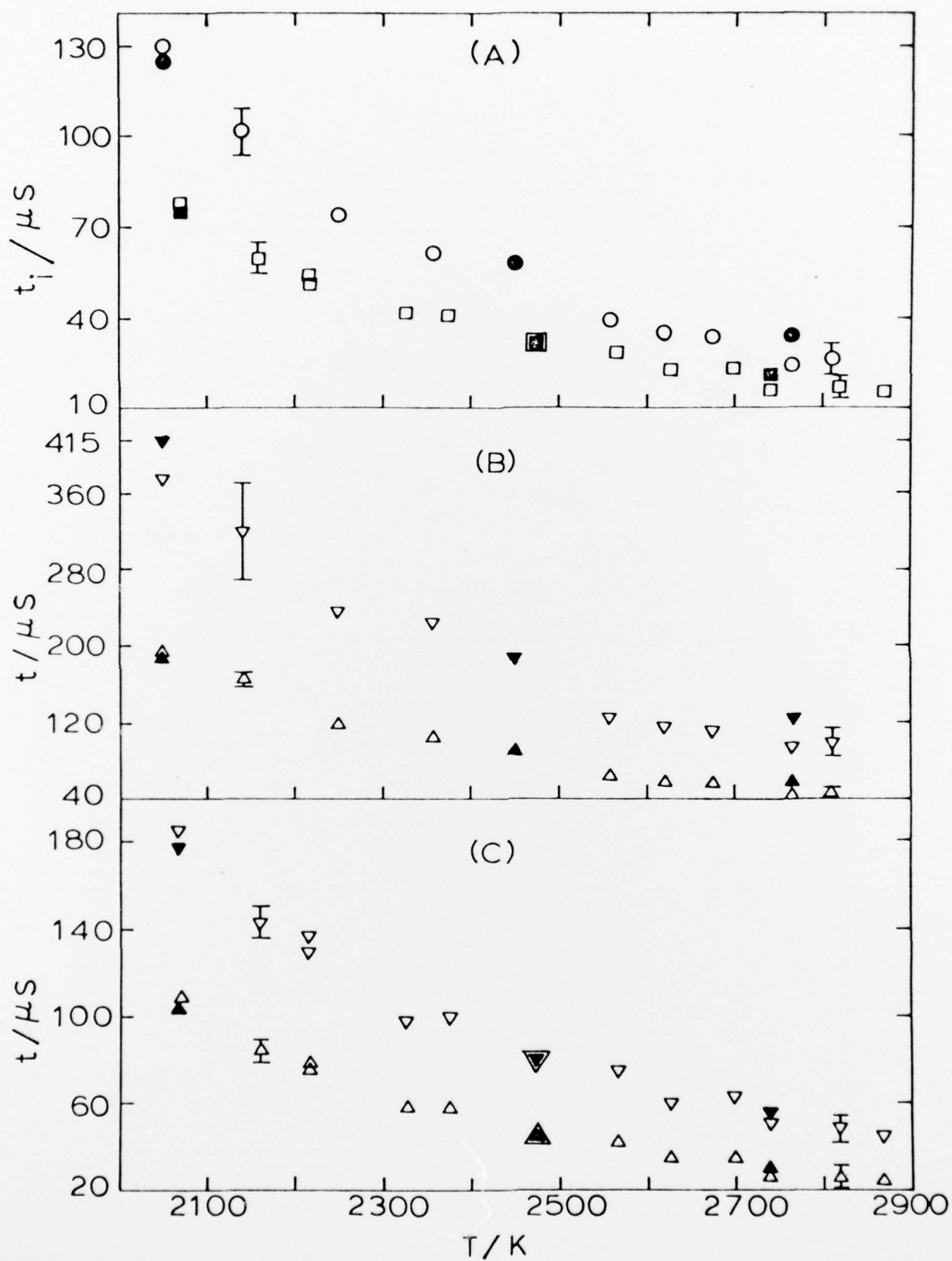


Fig. 4

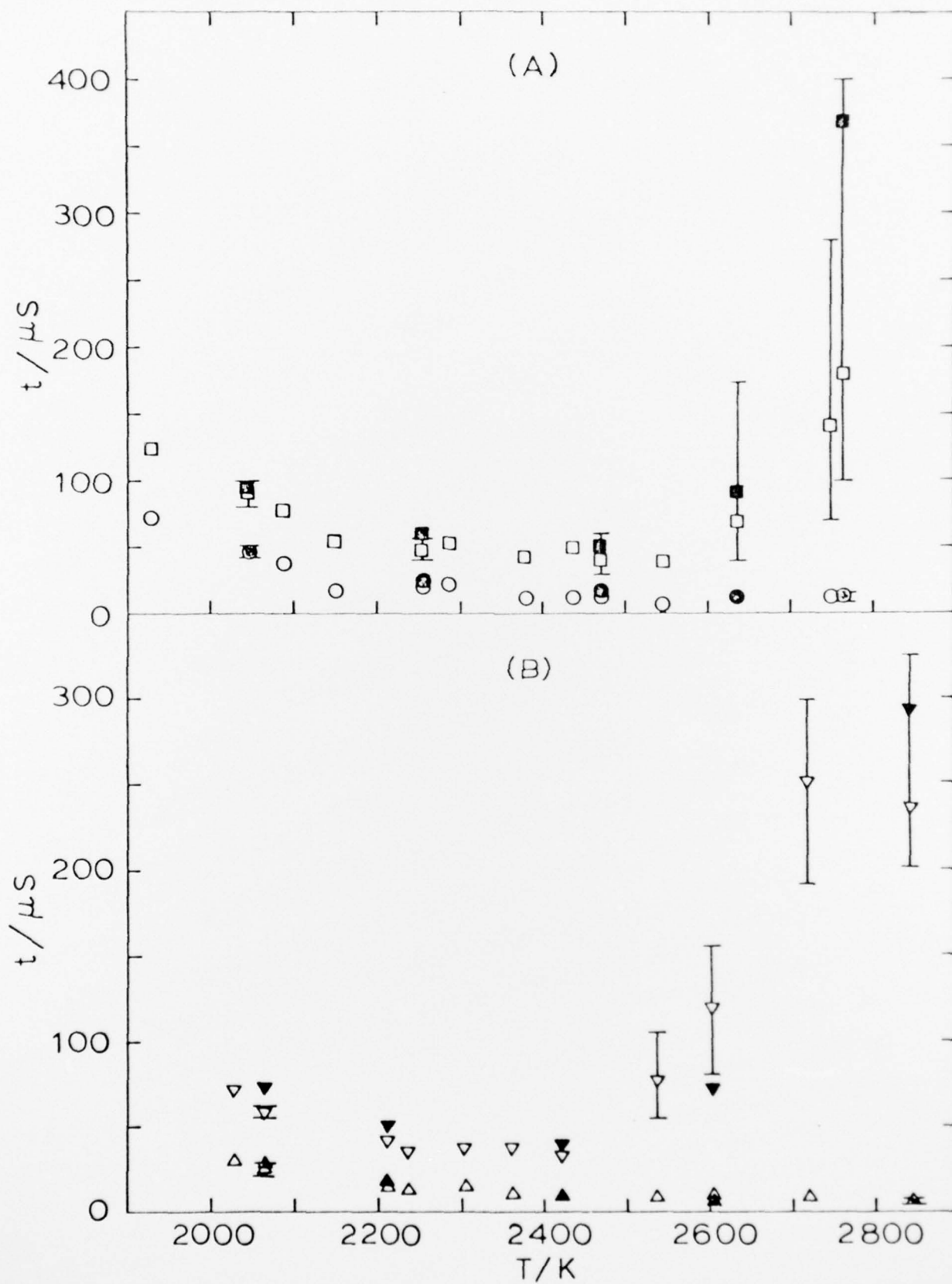


Fig. 5

DISTRIBUTION LIST

GOVERNMENT AGENCIES

1. British Embassy
3100 Massachusetts Avenue, N.W.
Washington, D.C. 20008
ATTN: Mr. J. Barry Jamieson
Propulsion Officer
2. Central Intelligence Agency
Washington, D.C. 20505
ATTN: CRS/ADD/Publications
3. Institute for Defense Analyses
400 Army-Navy Drive
Arlington, Virginia 22202
ATTN: Dr. Hans G. Wolfhard,
Sen. Staff
4. Defense Documentation Center
Cameron Station
Alexandria, Virginia 22314
5. EPA Technical Center
Research Triangle Park
North Carolina 27711
ATTN: Dr. W. Herget, P-222
6. Esso Research and Engineering Company
Government Research Laboratory
P.O. Box 8
Linden, New Jersey 07036
ATTN: Dr. William F. Taylor
7. Arnold Air Force Station
Tennessee 36389
ATTN: AEDC (DYF)
8. Arnold Air Force Station
Tennessee 37389
ATTN: R.E. Smith, Jr., Chief
T-Cells Division
Engine Test Facility
9. Air Force Aero Propulsion Laboratory
Wright-Patterson Air Force Base
Ohio 45433
ATTN: STINFO Office
10. Air Force Eastern Test Range
MU-135
Patrick Air Force Base
Florida 32925
ATTN: AFETR Technical Library
11. Air Force Office of Scientific Research
Boiling Air Force Base, Building 410
Washington, D.C. 20332
ATTN: Dr. Joseph F. Masi
12. Air Force Aero Propulsion Laboratory
Wright-Patterson AFB, Ohio 45433
ATTN: AFAPL/TBC
Dr. Kervyn Mach
13. Air Force Aero Propulsion Laboratory
Wright-Patterson AFB, Ohio 45433
ATTN: AFAPL/TBC
Francis R. Ostdiek
14. Air Force Rocket Propulsion Laboratory
Department of Defense
Edwards AFB, California 93523
ATTN: LKCG (Mr. Selph)
15. U.S. Army Air Mobility Research and
Development Laboratory
Eustis Directorate
Fort Eustis, Virginia 23604
ATTN: Propulsion Division
(SAVDL-EU-PP)
16. U.S. Army Artillery Combat
Developments Agency
Fort Sill, Oklahoma 73503
ATTN: Commanding Officer
17. U.S. Army Missile Command
Redstone Arsenal, Alabama 35809
ATTN: AMSM-RR
18. U.S. Army Missile Command
Redstone Scientific Information Center
Redstone Arsenal, Alabama 35809
ATTN: Chief, Document Section
19. Indiana State Library
140 North Senate Avenue
Indianapolis, Indiana 46204
ATTN: Patricia Matkovic
Reference Librarian
Indiana Division
20. NASA Headquarters
600 Independence
Washington, D.C. 20546
ATTN: Dr. Gordon Banerian
21. NASA Headquarters
Aeronautical Propulsion Division
Code RL, Deputy Director
Office of Advanced Research & Technology
Washington, D.C. 20546
ATTN: Mr. Nelson F. Rekos
22. NASA Ames Research Center
Deputy Chief Aeronautics Division
Mail Stop 27-4
Moffett Field, California 94035
ATTN: Mr. Edward W. Perkins
23. NASA Ames Research Center
Aerodynamics Branch 227-8
Moffett Field, California 94305
ATTN: Mr. Ira R. Schwartz
24. NASA Lewis Research Center
21000 Brookpark Road
Cleveland, Ohio 44135
ATTN: D. Morris, Mail Stop 60-3
25. NASA Lewis Research Center
Hypersonic Propulsion Section
Mail Stop 6-1
21000 Brookpark Road
Cleveland, Ohio 44135
ATTN: Dr. Louis A. Povinelli
26. NASA Marshall Space Flight Center
S&E ASTN-P
Huntsville, Alabama 35812
ATTN: Mr. Keith Chandler
27. National Science Foundation
Engineering Energetics
Engineering Division
Washington, D.C. 20550
ATTN: Dr. George Lee
28. National Science Foundation
Engineering Energetics
Engineering Division
Washington, D.C. 20550
ATTN: Dr. M. Ojalvo
29. National Science Foundation
Engineering Energetics
Engineering Division
Washington, D.C. 20550
ATTN: Dr. Royal Postenbach
30. Naval Air Development Center
Commanding Officer (AD-5)
Warminster, Pennsylvania 18974
ATTN: NADC Library
31. Naval Air Propulsion Test Center (R&T)
Trenton, New Jersey 08628
ATTN: Mr. Al Martino

32. Naval Air Systems Command
Department of the Navy
Washington, D.C. 20360
ATTN: Research Administrator
AIR 310
33. Naval Air Systems Command
Department of the Navy
Washington, D.C. 20360
ATTN: Propulsion Technology Admin.
AIR 330
34. Naval Air Systems Command
Department of the Navy
Washington, D.C. 20360
ATTN: Technical Library Division
AIR 604
35. Naval Ammunition Depot
Research and Development Department
Building 190
Crane, Indiana 47522
ATTN: Mr. B.E. Douda
36. Naval Ordnance Laboratory Commander
White Oak
Silver Springs, Maryland 20910
ATTN: Library
37. Naval Ordnance Systems Command
Department of the Navy
Washington, D.C. 20360
ATTN: ORD 0331
38. Naval Postgraduate School
Department of Aeronautics, Code 57
Monterey, California 93940
ATTN: Dr. Allen E. Fuhs
39. Naval Postgraduate School
Library (Code 2124)
Monterey, California 93940
ATTN: Superintendent
40. Naval Postgraduate School
Monterey, California 93940
ATTN: Library (Code 0212)
41. Office of Naval Research Branch Office
1030 East Green Street
Pasadena, California 91106
ATTN: Dr. Rudolph J. Marcus
42. Office of Naval Research Branch Office
536 South Clark Street
Chicago, Illinois 60605
ATTN: Commander
43. Office of Naval Research Branch Office
495 Summer Street
Boston, Massachusetts 02210
ATTN: Commander
44. Office of Naval Research
Power Branch, Code 473
Department of the Navy
Arlington, Virginia 22217
45. Office of Naval Research
Fluid Dynamics Branch, Code 438
Department of the Navy
Washington, D.C. 22217
ATTN: Mr. Morton Cooper
46. Naval Research Lab
Code 7710
Washington, D.C. 20390
ATTN: W.W. Balwanz
47. Naval Research Laboratory Director
Washington, D.C. 20390
ATTN: Technical Information Division
48. Naval Research Laboratory Director
Washington, D.C. 20390
ATTN: Library Code 2629 (ONRL)
49. Naval Ship Research and Development Center
Annapolis Division
Annapolis, Maryland 21402
ATTN: Library, Code A214
50. Naval Ship Systems Command
Department of the Navy
Washington, D.C. 20360
ATTN: Technical Library
51. Naval Weapons Center Commander
China Lake, California 93555
ATTN: Airbreathing Propulsion Branch
Code 4583
52. Naval Weapons Center
Chemistry Division
China Lake, California 93555
ATTN: Dr. William S. McEwan
Code 605
53. Naval Weapons Center
Commander
China Lake, California 93555
ATTN: Technical Library
54. Naval Weapons Center
Code 008, Thermochimistry Group
China Lake, California 93555
ATTN: Mr. Edward W. Price, Head
55. Naval Weapons Laboratory
Dahlgren, Virginia 22448
ATTN: Technical Library
56. Naval Undersea Research and
Development Center
San Diego, California 92132
ATTN: Technical Library
Code 13110
57. Naval Underwater Systems Center
Fort Trumbull
New London, Connecticut 06320
ATTN: Technical Library
58. Naval Underwater Systems Center
Code 5B-331
Newport, Rhode Island 02840
ATTN: Dr. Robert Lazar
59. Picatinny Arsenal
Commanding Officer
Dover, New Jersey 07801
ATTN: Technical Information Library
60. State Documents Section
Exchange and Gift Division
Washington, D.C. 20540
ATTN: Library of Congress
61. AeroChem Research Laboratories, Inc.
P.O. Box 12
Princeton, New Jersey 08540
ATTN: Dr. Arthur Fontijn
62. AeroChem Research Laboratories, Inc.
P.O. Box 12
Princeton, New Jersey 08540
ATTN: Library
63. Aerojet Liquid Rocket Company
P.O. Box 13222
Sacramento, California 95813
ATTN: Technical Information Center
64. Aeronautical Research Association
of Princeton
50 Washington Road
Princeton, New Jersey 08540
ATTN: Dr. C. Donaldson
65. Aeroprojects, Inc.
West Chester
Pennsylvania 19380

U.S. INDUSTRIES AND LABORATORIES

66. The Aerospace Corporation
P.O. Box 92957
Los Angeles, California 90009
ATTN: Mr. Alexander Muraszew
67. Atlantic Research Corporation
5390 Cherokee Avenue
Alexandria, Virginia 22314
ATTN: Dr. Andrej Macek
68. Atlantic Research Corporation
5390 Cherokee Avenue
Alexandria, Virginia 22314
ATTN: Librarian
69. Atlantic Research Corporation
5390 Cherokee Avenue
Alexandria, Virginia 22314
ATTN: Dr. Kermit E. Woodcock
Manager, Propulsion
70. Avco Everett Research Laboratory
Everett, Massachusetts 02149
ATTN: Librarian
71. Avco Lycoming Corporation
550 South Main Street
Stratford, Connecticut 06497
ATTN: Mr. John W. Schrader
72. Ballistics Research Laboratory
Commanding Officer
Aberdeen Proving Ground, Maryland 21005
ATTN: Librarian
73. Battelle
Columbus Laboratories
505 King Avenue
Columbus, Ohio 43201
ATTN: Mr. Abbott A. Putnam
Atmospheric Chemistry &
Combustion Systems Division
74. Beech Aircraft Corporation
9709 East Central
Wichita, Kansas 67201
ATTN: William M. Byrne, Jr.
75. Cell Aerospace Company
P.O. Box 1
Buffalo, New York 14240
ATTN: Technical Library
76. Bureau of Mines
Bartlesville Energy Research Center
Box 1396
Bartlesville, Oklahoma 74003
77. Calspan Corporation
4455 Genessee Street
Buffalo, New York 14221
ATTN: Head Librarian
78. Computer Genetics Corporation
Wakefield, Massachusetts 01880
ATTN: Mr. Donald Leonard
Technical Director
79. Convair Aerospace Division
Manager of Propulsion
P.O. Box 748
Fort Worth, Texas 76101
ATTN: L. H. Schreiber
80. Detroit Diesel Allison Division
P.O. Box 894
Indianapolis, Indiana 46206
ATTN: Dr. Sanford Fleeter
81. Dynalysis of Princeton
20 Nassau Street
Princeton, New Jersey 08540
ATTN: Dr. H.J. Herring
82. Fairchild Industries
Fairchild Republic Division
Farmingdale, New York 11735
ATTN: Engineering Library
83. Flame Research, Inc.
P.O. Box 10502
Pittsburgh, Pennsylvania 15235
ATTN: Dr. John Mantion
84. Forest Fire and Engineering Research
Pacific Southwest Forest & Range
Experiment Station
P.O. Box 245
Berkeley, California 94701
ATTN: Assistant Director
85. Garrett Corporation
AllResearch Manufacturing Company
Sky Harbor Airport
402 South 36th Street
Phoenix, Arizona 85034
ATTN: Mr. Aldo L. Romanin, Mgr.
Aircraft Propulsion Engine
Product Line
86. General Dynamics
Electro Dynamic Division
P.O. Box 2507
Pomona, California 91766
ATTN: Library MZ 620
87. General Dynamics
P.O. Box 748
Fort Worth, Texas 76101
ATTN: Technical Library MZ 2246
88. General Electric Company
AEG Technical Information Center
Mail Drop N-32, Building 700
Cincinnati, Ohio 45215
ATTN: J.J. Brady
89. General Electric Company
SPO-Bldg, 174AE
1000 Western Avenue
West Lynn, Massachusetts 01910
ATTN: Mr. W. Bruce Gist
90. General Electric Space Sciences Lab
Valley Forge Space Technology Center
Room N-9144
P.O. Box 8555
Philadelphia, Pennsylvania 19101
ATTN: Dr. Theodore Baure
91. General Motors Corporation
Detroit Diesel Allison Division
P.O. Box 894
Indianapolis, Indiana 46206
ATTN: Mr. P.C. Tram
92. General Motors Technical Center
Passenger Car Turbine Development
General Motors Engineering Staff
Warren, Michigan 48090
ATTN: T.F. Nagey, Director
93. Grumman Aerospace Corporation
Manager Space Vehicle Development
Bethpage, New York 11714
ATTN: Mr. O.S. Williams
94. Mr. Daniel L. Harshman
11131 Embassy Drive
Cincinnati, Ohio 45240
95. Hercules Incorporated
Allegany Ballistics Laboratory
P.O. Box 210
Cumberland, Maryland 21502
ATTN: Mrs. Louise S. Derrick
Librarian
96. Hercules Incorporated
P.O. Box 98
Magna, Utah 84044
ATTN: Library 100-H

97. LTV Vought Aeronautics Company
Flight Technology, Project Engineer
P.O. Box 5907
Dallas, Texas 75222
ATTN: Mr. James C. Utterback
98. Lockheed Aircraft Corporation
Lockheed Missiles and Space Company
Huntsville, Alabama 35804
ATTN: John M. Banefield
Supervisor Propulsion
99. Lockheed-Georgia Company
Dept. 72-47, Zone 259
Marietta, Georgia 30060
ATTN: William A. French
100. Lockheed Missiles and Space Company
2251 Hanover Street
Palo Alto, California 94304
ATTN: Palo Alto Library 52-52
101. Lockheed Propulsion Company
Scientific and Technical Library
P.O. Box 111
Redlands, California 92373
ATTN: Head Librarian
102. Los Alamos Scientific Laboratory
P.O. Box 1663
Los Alamos, New Mexico 97544
ATTN: J. Arthur Freed
103. The Marquardt Company
CCI Aerospace Corporation
16555 Saticoy Street
Van Nuys, California 91409
ATTN: Library
104. Martin-Marietta Corporation
P.O. Box 179
Denver, Colorado 90201
ATTN: Research Library 6617
105. Martin-Marietta Corporation
Orlando Division
P.O. Box 5837
Orlando, Florida 32805
ATTN: Engineering Library, mp-30
106. McDonnell Aircraft Company
P.O. Box 516
St. Louis, Missouri 63166
ATTN: Research & Engineering Library
Dept. 218 - Bldg. 101
107. McDonnell Douglas Corporation
Project Propulsion Engineer
Dept. 243, Bldg. 66, Level 25
P.O. Box 516
St. Louis, Missouri 63166
ATTN: Mr. William C. Paterson
108. McDonnell Douglas Astronautics Company
5301 Bolsa Avenue
Huntington Beach, California 92647
ATTN: A3-328 Technical Library
109. Nielsen Engineering and Research, Inc.
510 Clyde Avenue
Mountain View, California 94040
ATTN: Dr. Jack N. Nielsen
110. Northrop Corporation
Ventura Division
1515 Rancho Conejo Boulevard
Newbury Park, California 91230
ATTN: Technical Information Center
111. Mr. J. Richard Perrin
16261 Darcia Avenue
Encino, California 91316
112. Philco-Ford Corporation
Aeronutronic Division
Ford Road
Newport Beach, California 92663
ATTN: Technical Information Center
113. Pratt and Whitney Aircraft
Project Engineer, Advanced
Military System
Engineering Department - 28
East Hartford, Connecticut 06108
ATTN: Mr. Donald S. Rudolph
114. Pratt and Whitney Aircraft Division
United Aircraft Company
400 South Main Street
East Hartford, Connecticut 06108
ATTN: Mr. Dana B. Waring
Manager-Product Technology
115. Pratt and Whitney Aircraft
Program Manager, Advanced
Military Engineer
Engineering Department - 28
East Hartford, Connecticut 06108
ATTN: Dr. Robert I. Strough
116. Pratt and Whitney Aircraft
Florida Research and Development Company
P.O. Box 2691
West Palm Beach, Florida 33402
ATTN: Mr. William R. Alley
Chief of Applied Research
117. Rocket Research Corporation
11441 Willow Road
Redmond, Washington 98052
ATTN: Thomas A. Groudie
118. Rocketdyne Division
North American Rockwell
6633 Canoga Avenue
Canoga Park, California 91304
ATTN: Technical Information Center
D 596-108
119. Sandia Laboratories
P.O. Box 969
Livermore, California 94550
ATTN: Dr. Dan Hartley, Div. 8115
120. Sandia Laboratories
Livermore, California 94550
ATTN: Robert Gallagher
121. Sandia Laboratories
P.O. Box 5800
Albuquerque, New Mexico 87115
ATTN: Technical Library, 3141
122. Solar
2200 Pacific Highway
San Diego, California 92112
ATTN: Librarian
123. Standard Oil Company (Indiana)
P.O. Box 400
Naperville, Illinois 60540
ATTN: R. E. Pritz
124. Stauffer Chemical Company
Richmond, California 94802
ATTN: Dr. J. H. Morgenthaler
125. Teledyne CAE
1330 Laskey Road
Toledo, Ohio 43601
ATTN: Technical Library
126. TRW Systems
One Space Park
Redondo Beach, California 90278
ATTN: Mr. F.E. Fendell (R1/1004)
127. TRW Systems Group
One Space Park
Bldg. 0-1 Room 2080
Redondo Beach, California 90278
ATTN: Mr. Donald H. Lee Manager
128. United Technologies Research Center
East Hartford, Connecticut 06108
ATTN: Librarian
129. Valley Forge Sapce Technology Center
P.O. Box 8555
Philadelphia, Pennsylvania 19101
ATTN: Dr. Bert Zauderer
130. Vought Missiles and Space Company
P.O. Box 6267
Dallas, Texas 75222
ATTN: Library - 3-41000

U.S. COLLEGES AND UNIVERSITIES

131. Boston College
Department of Chemistry
Chestnut Hill, Massachusetts 02167
ATTN: Rev. Donald MacLean, S.J.
Associate Professor
132. Brown University
Division of Engineering
Box D
Providence, Rhode Island 02912
ATTN: Dr. R. A. Dobbins
133. California Institute of Technology
Department of Chemical Engineering
Pasadena, California 91109
ATTN: Professor W. H. Corcoran
134. California Institute of Technology
Jet Propulsion Laboratory
4800 Oak Grove Drive
Pasadena, California 91103
ATTN: Library
135. University of California, San Diego
Dept. of Engineering Physics
P.O. Box 109
La Jolla, California 92037
ATTN: Professor S.S. Penner
136. University of California
School of Engineering and Applied Science
7513 Boelter Hall
Los Angeles, California 90024
ATTN: Engineering Reports Group
137. University of California
Lawrence Radiation Laboratory
P.O. Box 808
Livermore, California 94550
ATTN: Technical Information Dept. L-3
138. University of California
General Library
Berkeley, California 94720
ATTN: Documents Department
139. Case Western Reserve University
10900 Euclid Avenue
Cleveland, Ohio 44106
ATTN: Sears Library - Reports Department
140. Case Western Reserve University
Division of Fluid Thermal and Aerospace Sciences
Cleveland, Ohio 44106
ATTN: Professor Eli Reshotko
141. Colorado State University
Engineering Research Center
Fort Collins, Colorado 80521
ATTN: Mr. V. A. Sandborn
142. The University of Connecticut
Department of Mechanical Engineering
U-139
Storrs, Connecticut 06268
ATTN: Professor E. K. Dabora
143. Cooper Union
School of Engineering and Science
Cooper Square
New York, New York 10003
ATTN: Dr. Wallace Chintz
Associate Professor of ME
144. Cornell University
Department of Chemistry
Ithaca, New York 14850
ATTN: Professor Simon H. Bauer
145. Franklin Institute Research Laboratories
Philadelphia, Pennsylvania 19103
ATTN: Dr. G.P. Wachtell
146. George Washington University
Washington, D.C. 20052
ATTN: Dr. Robert Goulard
Dept. of Civil, Mechanical and Environmental Engineering
147. George Washington University Library
Washington, D.C. 20006
ATTN: Reports Section
148. Georgia Institute of Technology
Atlanta, Georgia 30332
ATTN: Price Gilbert Memorial Library
149. Georgia Institute of Technology
School of Aerospace Engineering
Atlanta, Georgia 30332
ATTN: Dr. Ben T. Zinn
150. University of Illinois
Department of Energy Engineering
Box 4348
Chicago, Illinois 60680
ATTN: Professor Paul H. Chung
151. University of Illinois
College of Engineering
Department of Energy Engineering
Chicago, Illinois 60680
ATTN: Dr. D. S. Hacker
152. The Johns Hopkins University
Applied Physics Laboratory
Johns Hopkins Road
Laurel, Maryland 20810
ATTN: Chemical Propulsion Information Agency
153. The Johns Hopkins University
Applied Physics Laboratory
Johns Hopkins Road
Laurel, Maryland 20810
ATTN: Document Librarian
154. The Johns Hopkins University
Applied Physics Laboratory
Johns Hopkins Road
Laurel, Maryland 20810
ATTN: Dr. A. A. Westenberg
155. University of Kentucky
Department of Mechanical Engineering
Lexington, Kentucky 40506
ATTN: Dr. Robert E. Peck
156. Massachusetts Institute of Technology
Department of Chemical Engineering
Cambridge, Massachusetts 02139
ATTN: Dr. Jack B. Howard
157. Massachusetts Institute of Technology
Libraries, Room 14 E-210
Cambridge, Massachusetts 02139
ATTN: Technical Reports
158. Massachusetts Institute of Technology
Room 10-408
Cambridge, Massachusetts 02139
ATTN: Engineering Technical Reports

FOREIGN INSTITUTIONS

159. Massachusetts Institute of Technology
Dept. of Mechanical Engineering
Room 3-350
Cambridge, Massachusetts 02139
ATTN: Dr. M. Cardillo
160. Massachusetts Institute of Technology
Dept. of Mechanical Engineering
Room 3-246
Cambridge, Massachusetts 02139
ATTN: Professor James Fay
161. Midwest Research Institute
425 Volker Boulevard
Kansas City, Missouri 64100
ATTN: Dr. T. A. Milne
162. New Mexico State University
Dept. of Mechanical Engineering
Box 3450
Las Cruces, New Mexico 88003
ATTN: Dr. Dennis M. Zallen
163. New York Institute of Technology
Wheatley Road
Old Westbury, New York 11568
ATTN: Dr. Fox
164. University of North Carolina
Periodicals and Serials Division
Drawer 870 Library
Chapel Hill, North Carolina 27514
ATTN: Mr. Stephen Berk
165. University of Notre Dame
Serials Record
Memorial Library
Notre Dame, Indiana 46556
ATTN: B. McIntosh
166. University of Notre Dame
College of Engineering
Notre Dame, Indiana 46556
ATTN: Dr. Stuart T. McComas
Assistant Dean for Research
and Special Projects
167. Ohio State University
Dept. of Chemical Engineering
140 West 19th Avenue
Columbus, Ohio 43210
ATTN: Dr. Robert S. Brodkey
168. The Pennsylvania State University
Room 207, Old Main Building
University Park, Pennsylvania 16802
ATTN: Office of Vice President
for Research
169. Princeton University
Dept. of Aerospace and Mechanical
Sciences
James Forrestal Campus
Princeton, New Jersey 08540
ATTN: Dr. Martin Summerfield
170. Princeton University
James Forrestal Campus Library
P.O. Box 710
Princeton, New Jersey 08540
ATTN: V. N. Simosko, Librarian
171. Rice University
Welch Professor of Chemistry
Houston, Texas 77001
ATTN: Dr. Joseph L. Franklin
172. University of Rochester
Dept. of Chemical Engineering
Rochester, New York 14627
ATTN: Dr. John R. Ferron
173. Stanford University
Dept. of Aeronautics and Astronautics
Stanford, California 94305
ATTN: Dr. Walter G. Vincenti
174. State University of New York - Buffalo
Dept. of Mechanical Engineering
228 Parker Engineering Building
Buffalo, New York 14214
ATTN: Dr. George Rudinger
175. Stevens Institute of Technology
Department of Mechanical Engineering
Castle Point Station
Hoboken, New Jersey 07030
ATTN: Professor Fred Sisto
176. University of Virginia
Department of Aerospace Engineering
School of Engineering and Applied Science
Charlottesville, Virginia 22901
ATTN: Dr. John E. Scott
177. University of Virginia
Science/Technology Information Center
Charlottesville, Virginia 22901
ATTN: Dr. Richard H. Austin
178. Yale University
Mason Laboratory
9 Hillhouse Avenue
New Haven, Connecticut 06520
ATTN: Professor Peter P. Wegener
179. A/S Kongsberg Vaapenfabrikk
Gas Turbine Division
3601 Kongsberg, NORWAY
ATTN: R.E. Stanley
Senior Aerodynamicist
180. Conservatoire National des Arts
et Metiers
292, Rue Saint-Martin
75141 Paris Cedex 03, FRANCE
ATTN: Professor J. Gossee
Chaire de Thermique
181. DFVLR-Forschungszentrum Göttingen
Institut für Strömungsmechanik
Abteilung Theoretische Gashydrodynamik
D-3400 Göttingen
Bunsenstrasse 10, GERMANY
ATTN: Professor Klaus Oswatitsch
182. Ecole Royale Militaire
30 Avenue de la Renaissance
Bruxelles B-1040, BELGIUM
ATTN: Professor Emile Tits
183. Fysisch Laboratorium
Fijksuniversiteit Utrecht
Sorbonnelaan, Utrecht,
THE NETHERLANDS
ATTN: Dr. F. Van der Valk
184. Imperial College
Department of Chemical Engineering
London SW7, ENGLAND
ATTN: Professor F. J. Weinberg
185. Imperial College of Science
and Technology
Department of Mechanical Engineering
Exhibition Road
London, SW7, ENGLAND
ATTN: Professor Gaydon
186. Imperial College of Science
and Technology
Department of Mechanical Engineering
Exhibition Road
London SW7, ENGLAND
ATTN: D. C. Spalding
- 187/1 Laboratoire de Mécanique des Fluides
36, Route de Dardilly, 36
B.P. No. 17
69130 Ecully, FRANCE
ATTN: G. Assassa

- 187/2 Laboratoire de Mécanique des Fluides
Ecole Centrale Lyonnaise
36, Route de Dardilly
69130 Ecully, FRANCE
ATTN: Dr. K. Papiliou
188. Ministry of Defense
Main Building, Room 2165
Whitehall Gardens
London SW1, ENGLAND
ATTN: Mr. L.D. Nicholson ED, idc
Vice Controller of Aircraft
Procurement Executive
189. Mitglied des Vorstands der Fried
Krump GmbH
43 Essen, Altendorferstrabe 103
GERMANY
ATTN: Professor Dr. -Ing.
Wilhelm Dettmering
190. National Aerospace (NLR)
Voorsterweg 31
Noord-Oost-Polder-Emmelord
THE NETHERLANDS
ATTN: Mr. F. Jaarsma
191. National Research Council
Division of Mechanical Engineering
Montreal Road, Ottawa
Ontario, CANADA K1A 0R6
ATTN: Dr. R.B. Whyte
192. Nissan Motor Co., LTD.
3-5-1, Momoi, Suginami-Ku
Tokyo, JAPAN 167
ATTN: Dr. Y. Toda
193. Norwegian Defense Research Establishment
Superintendent NDRE
P.O. Box 25
2007 Kjeller, NORWAY
ATTN: Mr. T. Krog
194. ONERA
Energie and Propulsion
29 Avenue de la Division Leclure
92 Chatillon sous Bagneux, FRANCE
ATTN: Mr. M. Barre
195. ONERA
Energie and Propulsion
29 Avenue de la Division Leclure
92 Chatillon sous Bagneux, FRANCE
ATTN: Mr. J. Fabri
196. ONERA
Energie and Propulsion
29 Avenue de la Division Leclure
92 Chatillon sous Bagneux, FRANCE
ATTN: Mr. Viaud
197. ONERA-BED
External Relations and Documentation
Department
29, Avenue de la Division Leclure
92320 Chatillon, sous Bagneux, FRANCE
ATTN: Mr. M. Salmon
198. Orta Dogu Teknik Universitesi
Mechanical Engineering Department
Ankara, TURKEY
ATTN: Professor H. Sezgen
199. Queen Mary College
Department of Mechanical Engineering
Thile Eld Road
London E1, ENGLAND
ATTN: Professor M. W. Thring
200. Rolls-Royce (1971) Limited
Derby Engine Division
P.O. Box 31
Derby DE2 8BJ
London, ENGLAND
ATTN: C. Freeman, Installation
Research Department
201. Rome University
Via Bradano 28
00199 Rome, ITALY
ATTN: Professor Gaetano Salvatore
202. Sener
Departament de Investigacion
Km. 22.500 de la antigua carretera
Madrid - Barcelona, SPAIN
ATTN: Mr. J. T. Diez Roche
203. Service Technique Aeronautique Moteurs
4 Avenue de la Parte d'Issy
75753 Paris Cedex 15, FRANCE
ATTN: Mr. M. Pianko, Ing. en chef
204. The University of Sheffield
Dept. of Chemical Engineering
and Fuel Technology
Mappin Street, Sheffield S1 3JD
ENGLAND
ATTN: Dr. Norman Chigier
205. Sophia University
Science and Engineering Faculty
Kioi 7 Tokyo-Chiyoda JAPAN 102
ATTN: Professor M. Susuki
206. The University of Sydney
Dept. of Mechanical Engineering
N.S.W. 2006
Sydney, AUSTRALIA
ATTN: Professor R. W. Bilger
207. Technical University of Denmark
Fluid Mechanics Department
Building 404 2800 Lyngby
DK-DENMARK
ATTN: Professor K. Refslund
208. University of Leeds
Leeds, ENGLAND
ATTN: Professor Dixon-Lewis
209. Université de Poitiers Laboratoire
D'energetique et de Detonique
(L.A. au C.N.R.S. No. 193)
ENSMA - 86034 Poitiers, FRANCE
ATTN: Professor N. Manson
210. University of Tokyo
Department of Reaction Chemistry
Faculty of Engineering
Bunkyo-ku
Tokyo, JAPAN 113
ATTN: Professor T. Hikita
211. Vrije Universiteit Brussel
Fac. Toeg. Wetensch.
A. Buyllaan 105
1050 Brussels, BELGIUM
ATTN: Ch. Hirsch
- PROJECT SQUID CONTRACTORS
1975-76 and 1976-77 (New)
212. AeroChem Research Laboratory, Inc.
Reaction Kinetics Group
P.O. Box 12
Princeton, New Jersey 08540
ATTN: Dr. Arthur Fontijn
213. Aeronautical Research Associates of
Princeton, Inc.
P.O. Box 2229
50 Washington Road
Princeton, New Jersey 08540
ATTN: Dr. Ashok K. Varma
214. California Institute of Technology
Div. of Engineering and
Applied Science
Mail Stop 205-50
Pasadena, California 91109
ATTN: Dr. Anatol Roshko
215. Case Western Reserve University
Div. of Fluid, Thermal and Aerospace
Sciences
Cleveland, Ohio 44106
ATTN: Dr. J.S. T'ien

216. Colorado State University
Engineering Research Center
Foothills Campus
Fort Collins, Colorado 80521
ATTN: Dr. Willy Z. Sadeh
217. General Electric Company
Corporate Research and Development
P.O. Box 8
Schenectady, New York 12301
ATTN: Dr. Marshall Lapp
218. Massachusetts Institute of Technology
Chemistry Department, Room 6-123
77 Massachusetts Avenue
Cambridge, Massachusetts 02139
ATTN: Dr. John Ross
219. Michigan State University
Department of Mechanical Engineering
East Lansing, Michigan 48824
ATTN: Dr. John Foss
220. Pennsylvania State University
Applied Research Laboratory
University Park, Pennsylvania 16802
ATTN: Dr. Edgar P. Bruce
221. Polytechnic Institute of New York
Department of Aerospace Engineering
and Applied Mechanics
Farmingdale, New York 11735
ATTN: Dr. Samuel Lederman
222. Southern Methodist University
Thermal and Fluid Sciences Center
Institute of Technology
Dallas, Texas 75275
ATTN: Dr. Roger L. Simpson
223. Stanford University
Mechanical Engineering Department
Stanford, California 94305
ATTN: Dr. James P. Johnston
224. Stanford University
Mechanical Engineering Department
Stanford, California 94305
ATTN: Dr. S. J. Kline
225. Stanford University
Mechanical Engineering Department
Stanford, California 94305
ATTN: Dr. Sidney Self
226. TRW Systems
Engineering Sciences Laboratory
One Space Park
Redondo Beach, California 90278
ATTN: Dr. J. E. Broadwell
227. United Technologies Research Center
400 Main Street
East Hartford, Connecticut 06108
ATTN: Mr. Franklin O. Carta
228. United Technologies Research Center
400 Main Street
East Hartford, Connecticut 06108
ATTN: Dr. Alan C. Eckbreth
229. University of California - San Diego
Department of Aerospace and
Mechanical Engineering
La Jolla, California 92037
ATTN: Dr. Paul Libby
230. University of Colorado
Department of Aerospace
Engineering Sciences
Boulder, Colorado 80304
ATTN: Dr. Mahinder S. Uberoi
231. University of Michigan
Department of Aerospace Engineering
Ann Arbor, Michigan 48105
ATTN: Dr. T. C. Adamson, Jr.
232. University of Michigan
Department of Aerospace Engineering
Ann Arbor, Michigan 48105
ATTN: Dr. Martin Sichel
233. University of Missouri - Columbia
Department of Chemistry
Columbia, Missouri 65201
ATTN: Dr. Anthony Dean
234. University of Southern California
Department of Aerospace Engineering
University Park
Los Angeles, California 90007
ATTN: Dr. F. K. Broward
235. University of Washington
Department of Mechanical Engineering
Seattle, Washington 98195
ATTN: Dr. F.B. Gessner
236. Virginia Polytechnic Institute and
State University
Mechanical Engineering Department
Blacksburg, Virginia 24601
ATTN: Dr. Walter F. O'Brien, Jr.
237. Virginia Polytechnic Institute and
State University
Mechanical Engineering Department
Blacksburg, Virginia 24061
ATTN: Dr. Hal L. Moses
238. Yale University
Engineering and Applied Science
Mason Laboratory
New Haven, Connecticut 06520
ATTN: Dr. John B. Fenn
239. School of Aeronautics and Astronautics
Grissom Hall
West Lafayette, Indiana 47907
ATTN: Library
240. School of Mechanical Engineering
Mechanical Engineering Building
West Lafayette, Indiana 47907
ATTN: Library
- 241-250. Purdue University Advisors

UNCLASSIFIED

SECURITY CLASSIFICATION OF THIS PAGE (When Data Entered)

REPORT DOCUMENTATION PAGE		READ INSTRUCTIONS BEFORE COMPLETING FORM
1. REPORT NUMBER SQUID-UM0-2-PU	2. GOVT ACCESSION NO.	3. RECIPIENT'S CATALOG NUMBER
4. TITLE (and Subtitle) A SHOCK TUBE STUDY OF THE H ₂ /O ₂ /CO/Ar AND H ₂ /N ₂ O/CO/Ar SYSTEMS.		5. TYPE OF REPORT & PERIOD COVERED Technical rept.
7. AUTHOR(s) Anthony M. Dean, Don C. Steiner and Edward E. Wang		6. PERFORMING ORG. REPORT NUMBER
9. PERFORMING ORGANIZATION NAME AND ADDRESS Department of Chemistry, University of Missouri-Columbia Columbia, Missouri 65201		8. CONTRACT OR GRANT NUMBER(s) N00014-75-C-1143, NR-098-038
11. CONTROLLING OFFICE NAME AND ADDRESS Project SQUID, Chaffee Hall Purdue University West Lafayette, Indiana 47907		10. PROGRAM ELEMENT, PROJECT, TASK AREA & WORK UNIT NUMBERS
14. MONITORING AGENCY NAME & ADDRESS (if different from Controlling Office) Office of Naval Research Department of the Navy Arlington, Virginia 22217		12. REPORT DATE May 1977
		13. NUMBER OF PAGES 44
		15. SECURITY CLASS. (of this report) Unclassified
		15a. DECLASSIFICATION/DOWNGRADING SCHEDULE
16. DISTRIBUTION STATEMENT (of this Report) This document has been approved for public release and sale; its distribution is unlimited.		
17. DISTRIBUTION STATEMENT (of the abstract entered in Block 20, if different from Report)		
18. SUPPLEMENTARY NOTES		
19. KEY WORDS (Continue on reverse side if necessary and identify by block number) Shock Tube H ₂ /O ₂ System H ₂ /N ₂ O System		
20. ABSTRACT (Continue on reverse side if necessary and identify by block number) Emissions at 450 nm and 4.27 μm have been measured when a variety of mixtures containing H ₂ , CO, either O ₂ or N ₂ O, and Ar were heated behind reflected shock waves to temperatures of 2000-2850 K and total concentrations near 5x10 ¹⁸ molecule/cm ³ . These emissions were used to obtain absolute concentration - time data for both oxygen atoms and carbon dioxide. The data were then compared to the results of numerical integrations of the likely mechanisms. It was observed that quantitative agreement between calculations and observations were obtained for the H ₂ /CO/O ₂ /Ar system using		

DD FORM 1 JAN 73 1473

EDITION OF 1 NOV 65 IS OBSOLETE
S/N 0102-014-6601

UNCLASSIFIED

SECURITY CLASSIFICATION OF THIS PAGE (When Data Entered)

403 617 * 5 x 10 to the 18th power molecules/cc 1B

Unclassified

SECURITY CLASSIFICATION OF THIS PAGE(When Data Entered)

recent high temperature literature rate constants. For the $H_2/CO/N_2O/Ar$ system, the rate constant for the reaction:



was adjusted so as to fit the data. Here it was found that a good fit to both $[O]$ and $[CO_2]$ profiles could be achieved with $k = 3.0 \times 10^{-9} \times \exp(-113kJ/RT) \text{ cm}^3/\text{molecule} \cdot \text{s}$. Comparison to data at lower temperatures suggests that this might be another example of a "non-Arrhenius" rate constant. The implications of these results to studies of hydrocarbon oxidation are discussed.

$\times 3 \times 10^{-9} \text{ to } -9^{\text{th}} \text{ power}$

SECURITY CLASSIFICATION OF THIS PAGE(When Data Entered)